Segmented Poly(tetramethylene oxide) Zwitterionomers and Their Homologous Ionenes. 3. Structural Study through SAXS and SANS Measurements

Bruno Grassl, André Mathis, Michel Rawiso, and Jean-Claude Galin*

Institut Charles Sadron, CNRS-ULP, 6, rue Boussingault, 67083 Strasbourg Cedex, France

Received June 18, 1996; Revised Manuscript Received November 19, 1996[⊗]

ABSTRACT: The structure in bulk of a series of segmented poly(tetramethylene oxide) (PTMO) zwitterionomers of the ammonioalkanesulfonate ($N^+(CH_2)_pSO_3^-$, $p = 3, 4$) or alkoxydicyanoethenolate ($N^+(CH_2)_pOCOC^-(CN)_2$, $p = 2, 3$) type and of their homologous ionenes was analyzed through small angle X-ray and neutron scattering measurements in their amorphous state. Segregation of the polar units from the PTMO matrix resulting in sharp interfaces systematically occurs in all the systems. These two-phase structures are thermally stable and still persist in the liquid state up to at least 140 and 100 °C for sulfonates and dicyanoethenolates, respectively. However, long range order is observed only in the case of zwitterionomers bearing a bifunctional junction, with a typical transition from a lamellar structure for the shorter PTMO segments ($M_n^0 \sim (1.8-2.2) \times 10^3$, high zwitterion density, lamellar spacings between 7 and 8 nm with a thickness of the zwitterionic layer of about 1 nm) to a hexagonal structure for the longer ones ($M_n^0 > 3.6 \times 10^3$, low zwitterion density, radius of the zwitterionic cylinder of about 1.2 nm). In the lamellar structure, supported by transmission electron microscopy which shows coherence domains spreading over more than 100 nm, the PTMO subchain is extended by about 50% with respect to its unperturbed dimensions. Such an extension does not occur in the less sterically constraining hexagonal structure. The swelling of the ammonioethoxydicyanoethenolate zwitterionomers by tetrahydrofuran, a selective solvent of the PTMO segments, results in physical gels (swelling ratios $Q \leq 5$) with a progressive loss of long range order. It involves either an inhomogeneous swelling process or a gradual fragmentation of the zwitterionic microdomains of constant and strongly anisotropic shape.

Introduction

In the two previous papers, we described the synthesis[1] and the structural characterization in bulk[2] (DSC, solid state ^{1}H-NMR spectroscopy) of a series of homologous segmented poly(tetramethylene oxide) zwitterionomers and ionenes of the general formula

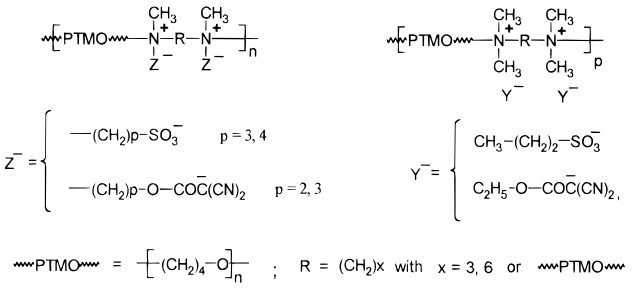

For PTMO block molecular weights higher than 3×10^3, isothermal crystallization from the melt at room temperature may be observed, but with very slow kinetics (over 1 week). In their amorphous state all these materials display a very typical biphasic morphology (two glass transitions) characterized by the dispersion of hard microdomains concentrating all the polar units and only a weak fraction of about 10−30% of the nonpolar PTMO segments (high-T_g phase) in a pure soft PTMO matrix (low-T_g phase). This two-phase structure is in very good agreement with the well-known ionomer morphology: see the multiplet-cluster concept recently revisited by Eisenberg et al.[3] or the microphase separation analyzed for multiblock copolymers $(A_xB_y)_n$ in the so-called "superstrong segregation regime" (very strongly self-interacting B blocks and very high Flory interaction parameter χ_{AB}) for the limiting case of one B unit per B block.[4] Strong dipolar or Coulombic interactions between the functionalized short segments result in their self-association in multiplets and in their segregation from the highly mobile ($T_g = -77$ °C) and nonpolar PTMO matrix (no possibility of efficient solvation of the zwitterionic or ion pair structures). The overlap of domains of reduced mobility defined by the multiplets and the few surrounding PTMO units directly anchored (about two or three PTMO units per zwitterion) leads to clusters of sufficient size (>10 nm) to show their own glass transition. The very strong cohesion of the multiplets is clearly shown by their persistence at temperatures well above the glass transition of the clusters. Comparison with statistical *n*-butyl acrylate zwitterionomers functionalized with the same dipolar units[5,6] points out two interesting differences: (i) the systematic presence of phase separation even for low polar unit contents while statistical copolymers appear monophasic in this composition range (zwitterion molar fraction <0.04); (ii) the quantitative and thus far better segregation of the dipolar units from the nonpolar matrix which appears never pure for statistical copolymers.

The main reason for such differences arises more likely from the very regular distribution of the dipolar units in the segmented chain than from the slightly higher mobility and the slightly lower polarity of the PTMO matrix. However, if DSC and solid state ^{1}H-NMR measurements have allowed a self-consistent and quantitative description of the segmented copolymers morphology in terms of relative importance and composition of the coexisting phases of different rigidity, the determination of the shape, size, polydispersity, and spatial organization of the polar microdomains remains an open question. In the most studied case of ionomers these problems have long been a much debated topic and cannot be still considered as definitely solved, even

[⊗] Abstract published in *Advance ACS Abstracts,* March 15, 1997.

S0024-9297(96)00880-7 CCC: $14.00

if two important features appear well ascertained: the polar multiplets are essentially dispersed in the nonpolar matrix according only to a liquidlike order[3,7−9] for statistical copolymers, and they cannot be identified with isotropic spherical micelles as shown by very recent theoretical calculations.[10] The main goal of the present work is thus to determine the type of structure and its geometrical parameters through small angle X-ray and neutron scattering experiments (SAXS and SANS, respectively) with special emphasis on three major points: (i) the search for long range order in these materials which may be highly favored by the regular segmented structure of the individual chains, as suggested by literature data on analogous segmented PTMO[11] or poly(propylene oxide) ionomers[12] and in segmented PTMO ionenes;[13,14] (ii) the analysis of the molecular architecture influence on the material morphology and on its average characteristic distances (PTMO segment and diamine lengths, zwitterion structure); (iii) the comparison of the efficiencies of zwitterionic and homologous ion-pair structures (identical structure for the cationic and anionic sites) for the development of microphase segregation and long range order: zwitterionomers versus ionenes.

The sample designation systematically used throughout the following text allows us to identify successively zwitterionomers (Z) or ionenes (I), the molecular weight of the PTMO block, zwitterions or ion pairs of the alkanesulfonate (S*p*) or alkoxydicyanoethenolate (E*p*) type with *p* methylene groups in the intercharge arm for zwitterionic structures, and finally, the number of methylene groups *x* in the short diamino segment:

$$\text{Z or I}[M_n^0(\text{PTMO})/100]\text{-S}p \text{ or E}p\text{-}x$$

Thus, sample Z22-E3-6 is a zwitterionomer carring PTMO segments of number average molecular weight 2200, functionalized with ammoniopropoxydicyanoethenolate structures separated by a short segment of six methylene groups. Sample I22-E-6 is the homologous ionene, where the figure *p* has been obviously deleted.

Experimental Section

Materials. The synthesis and molecular characterization of the various PTMO zwitterionomers and ionenes were described previously:[1] the weight average degree of polycondensation of the PTMO blocks ($M_w^0/M_n^0 < 1.15$) in the segmented chain is never lower than 15, and the polydispersity index of the copolymers is about 2. The samples were molded at 120 °C for 8 h under a pressure of 10^4 Pa, after a progressive heating at a rate of about 1 °C·min^{-1}. They were obtained in the form of homogeneous and fairly transparent disks of diameter 34 mm and of controlled thickness in the range 0.2−2 mm (±0.02 mm). All the molded samples were annealed at 60 °C under vacuum (<0.1 mbar) for at least 4 h before any scattering measurements. For swelling experiments, a given amount of material was cut in the disks and directly placed in the scattering cell under an atmosphere saturated with tetrahydrofuran vapor. The swelling ratios could be easily monitored through the sorption times and measured by weighing. The volume fractions of the various components in all the pure or swelled copolymers under investigation were derived from their weight fractions and their specific volumes by assuming simple additivity v(25 °C) = 0.780, 1.018, and 1.128 mL·g^{-1} for the polar short segments,[15] the amorphous PTMO segments,[16] and THF, respectively.

Wide- and Small-Angle X-ray Scattering Measurements. They were performed between 20 and 140 °C using an experimental device[17] operating with a linear collimation (infinite height slit conditions) of a monochromatic X-ray beam of $\lambda = 0.154$ nm (Cu Kα_1). Photographic films were used for WAXS measurements (Guinier camera) and a linear detector for SAXS measurements. In the latter case, the configuration of the experimental device allows us to cover a range of scattering vectors q between 0.03 and 3 nm^{-1} ($q = (4\pi/\lambda)\sin\theta$ where 2θ is the scattering angle).

Small-Angle Neutron Scattering Measurements. They were performed at room temperature, on the PAXE spectrometer of the Laboratoire Leon Brillouin (LLB, Saclay, France). It operates with a pinhole collimation and a bidimensional detector. Two experimental configurations (wavelength λ and sample−detector distance D: $\lambda = 1.0$ nm, $D = 3$ m and $\lambda = 0.6$ nm, $D = 1$ m) were used in order to cover a broad q range, $0.0651 < q\ (\text{nm}^{-1}) < 4.26$. The width of the wavelength distribution corresponds to $\Delta\lambda/\lambda = 10\%$.

The values of the contrast between the nonpolar (A) and polar (B) units, arising from the difference between their scattering length densities ρ_A and ρ_B, $(\rho_B - \rho_A)^2$, are calculated in the usual way. They are always high enough, in the range $(4.84-7.84) \times 10^{-20}$ cm^{-4}, to allow reliable SAXS measurements for all the copolymers, while only zwitterionomers or ionenes of the alkoxydicyanoethenolate type may be proned to SANS measurements: compare $(\rho_B - \rho_A)^2 \sim (2.25-6.76) \times 10^{-20}$ cm^{-4} for dicyanoethenolates with $(\rho_B - \rho_A)^2 \sim (0.04-0.81) \times 10^{-20}$ cm^{-4} for sulfonates.

Data Treatment. The data were treated according to current procedures for small angle isotropic scattering.[18,19] Assuming a q independent background, we have checked that the coherent differential cross section containing all the structural information, $I(q)$, decreases at large q values according to the classical q^{-4} or q^{-3} dependence for pinhole (SANS) or linear (SAXS) collimation. This Porod's law[19,20] was thus used to perform an exact background subtraction. For neutron scattering, the data were also put on an absolute scale with an accuracy better than 10%. Because we are concerned with microdomains having a well-defined geometry or flat interfaces, as indicated by the observation of the characteristic Porod law at high q values, the normalization of data was carried out by using the relations[20]

$$I(q) = (\rho_B - \rho_A)^2 \Phi_B G(q,c) \tag{1}$$

$$G(q,c) = G(q)\, S(q) \tag{2}$$

where ρ_A and ρ_B are the scattering length densities of PTMO and zwitterionic media, respectively, Φ_B is the zwitterionic volume fraction. $G(q)$ is the form factor of the zwitterionic microdomains, related to the dimensionless form factor $P(q)$ such as $P(q=0) = 1$ by the relation

$$G(q) = V_p P(q) \tag{3}$$

where V_p represents the volume of the zwitterionic particles. $S(q)$ is the dimensionless structure factor that contains the information related to the organization of the microdomains. For samples exhibiting a translational order, it reduces to Bragg peaks; for samples exhibiting a liquidlike order, its limiting behaviors are

$$S(q)_{q=0} = k_B T\left[\left(\frac{\partial \pi}{\partial \Phi}\right)_T\right]^{-1} \qquad \text{and} \qquad S(q)_{q\to\infty} = 1 \tag{4}$$

where π is the osmotic pressure, T is the temperature, and k_B is the Boltzmann constant.

At high q values, according to the Porod law we have

$$q^4 I(q) = (\rho_B - \rho_A)^2 2\pi \frac{S}{V} = H_1 \tag{5}$$

where S/V is the total interfacial area per unit volume.

Such a behavior can also be written

$$q^4 G(q) = 2\pi \frac{S_p}{V_p} = H_2 \tag{6}$$

where S_p and V_p are the number average surface and volume of the scattering zwitterionic particles, respectively.

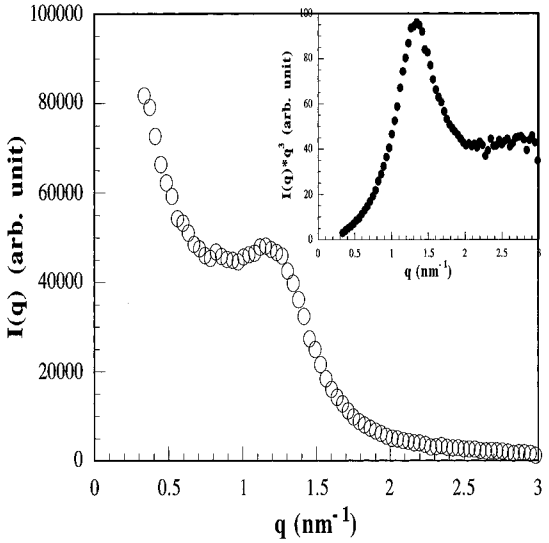

Figure 1. SAXS pattern of ionene I19-S-6.

Transmission Electron Microscopy (TEM). The measurements were performed on a Zeiss CEM 902 microscope operating at 80 kV, in the Elf-Atochem Research Laboratories (Serquigny). Samples were studied as thin films of thickness in the range 50−60 nm, obtained by ultracryotomy at −100 °C. They were stained by ruthenium tetroxide in the vapor phase for 45 s.

Results and Discussion

For all the segmented copolymers, the lack of any Bragg peak typical of crystalline PTMO[16] in the WAXS patterns shows that the copolymers may be safely assumed completely amorphous, as a result of their thermal history just before X-ray measurements (see Experimental Section). Moreover, the lack of any other sharp diffraction peak in the same q range strongly suggests the lack of any well-defined order within the polar scattering domains (see further discussion).

Overview of the Heterogeneous Structure, of the Interface Sharpness, and of the Thermal Stability of the Polar Aggregates. The SAXS patterns systematically show strong scattering typical of heterogeneous materials, but with very significant differences according to the chain chemical structure, as shown in Figures 1 and 2. The Porod representation added in the same figures allows us first to better reveal the higher order scattering peaks and second to show that the system does involve interfaces (behavior at high q values). They range from single broad peak diagrams for the ionenes, much like in the most usual ionomers, to multipeak diagrams (two peaks in most cases) for the zwitterionomers, correlated with the existence of long range order in these latter materials. An estimation of the interface thickness in these biphasic copolymers was performed according to the classical Porod analysis of the SAXS profiles at high q values according to $I(q) \propto q^{-3} \exp(-\sigma^2 q^2)$ for $q > 2$ nm^{-1} with $t = \sqrt{2\pi}\sigma$, where $I(q)$ is the scattered intensity and t is the interface thickness. The Porod plot of the experimental data of the zwitterionomer Z20-E3-6 given in Figure 3 is quite representative of the various polymers. In our experimental conditions ($q_{max} \approx 6$ nm^{-1}) the maximum spatial resolution is about 1 nm, and at this scale, the interface is sharp. Comparison with literature data on analogous PTMO ionenes of similar PTMO length ($M_n^0 \sim 1.8 \times 10^3$) carrying various halides (Cl^-, Br^-, I^-) as counterions is somewhat puzzling: the interface thickness

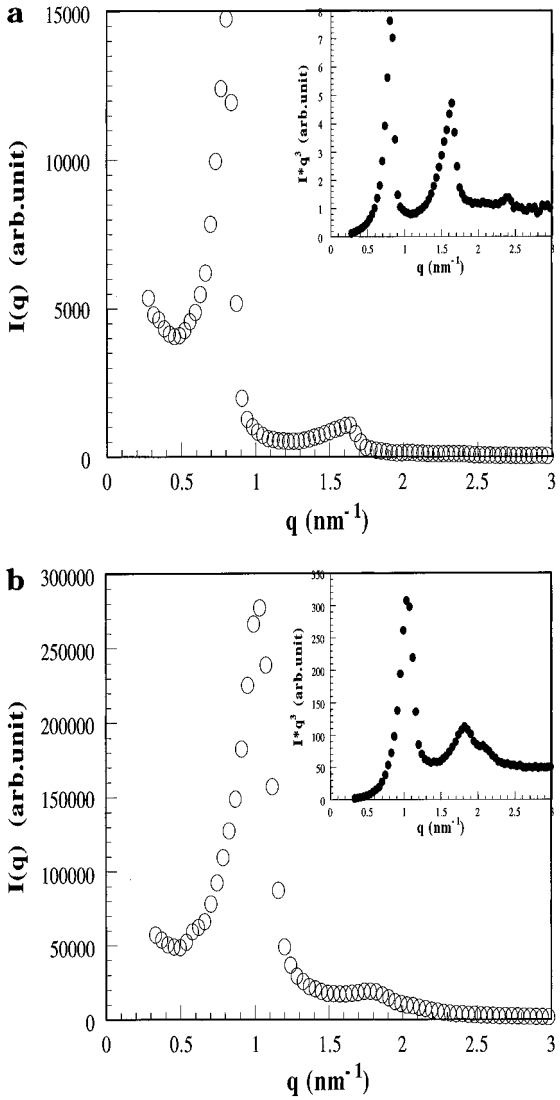

Figure 2. SAXS patterns of two representative zwitterionomers: (a) Z20-S3-6 (three diffraction orders in the ratios 1:2:3, lamellar structure); (b) Z17-S3-3 (three diffraction orders in the ratios 1:$\sqrt{3}$:2, hexagonal structure).

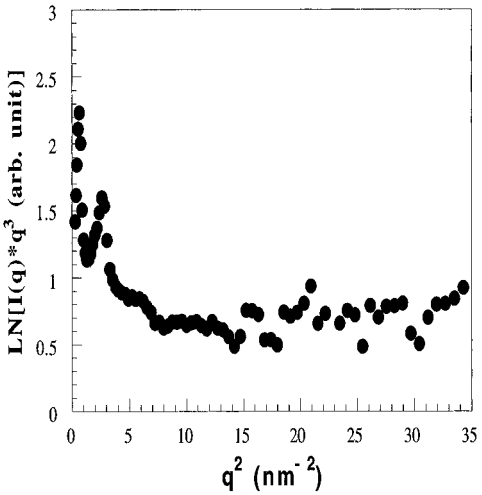

Figure 3. SAXS data of zwitterionomer Z20-S3-6 plotted for the determination of the interface thickness.

measured in the same way drastically increases from 0.1−0.2 to 1.1−1.2 nm when going from 1,4-bis((dimethylammonio)methyl)benzene[21] to bipyridinium[14] short segments. The reliability of the first very low values

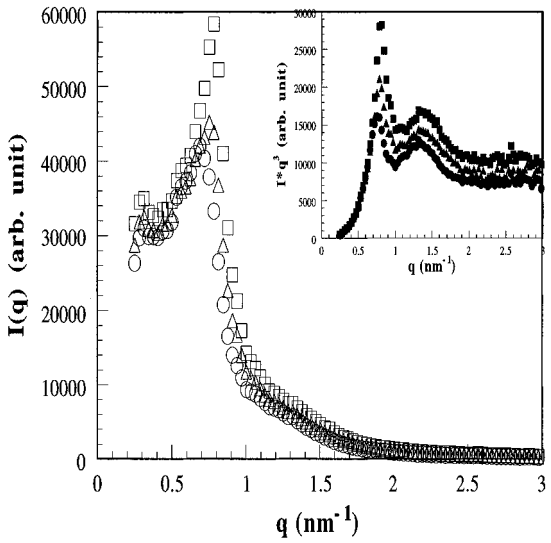

Figure 4. SAXS pattern of zwitterionomer Z52-S3-6 at various temperatures: (●) 25 °C; (▲) 80 °C; (■) 140 °C.

Table 1. SAXS Analysis and Characteristics Dimensions of the Polar Domains (Thickness *e* and Radius *R* of the Polar Layer or Cylinder in Lamellar or Hexagonal Structures, and Surface *S* Available per PTMO Segment at the Interface) of the Various Zwitterionomers and Ionenes

sample	Φ_B	d (nm)	e or R (nm)	S (nm^2)
Lamellar Structure[a] (e)				
Z22-E2-6	0.124	7.2	0.9	0.60
Z17-E2-3	0.143	6.7	1.0	0.51
Z20-E3-6	0.147	8.1	1.2	0.48
Z20-S3-6	0.128	7.4	0.9	0.51
Z20-S4-6	0.130	7.9	1.0	0.47
Hexagonal Structure[b] (R)				
Z36-E2-6	0.089	8.1	1.4	0.73
Z52-E2-6	0.055	8.7	1.2	0.87
Z67-E2-6	0.046	8.5	1.1	0.94
Z37-S3-6	0.074	7.6	1.3	0.78
Z52-S3-6	0.053	8.0	1.2	0.87
Z67-S3-6	0.042	8.2	1.0	0.96
Z17-S3-3	0.133	6.3	1.4	0.63
Liquid Order				
Z19-E2	0.063	5.1	1.3	0.51
Z19-S3	0.057	5.1	1.2	0.48
I19-E-6	0.153	7.0	2.3	0.75
I19-S-6	0.146	4.9	1.6	1.01
I19-T-6[c]	0.141	8.2	2.7	0.69

[a] Bragg spacing ratios d_1:d_2 = 2.00 ± 0.06. [b] Bragg spacing ratios d_1:d_2 = 1.73 ± 0.03. [c] Ionene precursor with triflate counterions.

may appear questionable, taking into account the experimental spatial resolution ($q_{max} \sim 4$ nm^{-1}).

Temperature effects were briefly studied on two representative zwitterionomers of the ammoniopropanesulfonate and ethoxydicyanoethenolate type, respectively. For the first copolymer Z52-S3-6, increasing the temperature from 20 to 140 °C (degradation under nitrogen only starts at T > 200 °C[1]) leads to the scattering curves given in Figure 4, and their variations are reversible with temperature. The Porod invariant $\int_0^\infty qI(q)\,dq$ (infinite height slit conditions), calculated within the range q = 0.25−3.0 nm^{-1}, slightly increases with temperature by about 30%. This trend reflects likely an increase of electronic contrast in this heterogeneous material. After correction of the intensities by the corresponding value of the Porod invariant at every temperature, all the scattering patterns become superposable. This very typical feature clearly shows that both the long range spatial organization of the scattering entities (position of the two peaks) and their shape and average dimensions (the constant plateau value at high q is directly correlated with their ratio surface/volume, S_p/V_p) are independent of temperature. In an alternative way, the ratio $\int_0^\infty I(q)\,dq/\int_0^\infty I(q)q\,dq$ allows us to calculate the characteristic correlation length L_c of the two-phase system. The constant value L_c = 2.66 ± 0.06 nm observed over the whole temperature range confirms the previous conclusion. Thus, going through the glass transition of the hard domains at about 44 °C, as previously derived from DSC measurements,[2] does not result in any structural reorganization. In a parallel way, temperature has no significant influence on the SAXS patterns in the dicyanoethenolate series for copolymer Z22-E2-6 heated to 100 °C, while the glass transition temperature of the hard domains occurs at about 25 °C.[2] This very high cohesion of the zwitterionic microdomains, already observed on statistical *n*-butyl acrylate zwitterionomers functionalized with identical structures,[5,6] results from the very strong dipolar interactions between zwitterions of unusually high dipole moments:[22,23] μ = 24−31 D for all the zwitterionic structures S-3, S-4 and E-2, E-3 in their fully extended conformation which is preferred in the zwitterionic aggregates.[23] The temperature behavior of these systems is typical of the so-called "superstrong segregation" regime.[4]

Determination of the Type of Long Range Order in the Zwitterionomers. For all the zwitterionomers, the type of long range order was first derived from the ratios of the Bragg spacings ($d = 2\pi/q$) corresponding to the multiple peak scattering patterns (generally, two peaks). The agreement in the d values directly measured on the crude scattering profiles $I(q)$, obtained either in SAXS or SANS experiments is good, the differences being always lower than 5%.

Only two zwitterionomers display three orders of diffraction in their SAXS patterns, as shown in Figure 2:

•Z20-E3-6, with Bragg spacings in the ratio 1:2:3, the first order corresponding to d = 8.1 nm: this behavior strongly suggests a lamellar structure, as already observed in some segmented PTMO ionenes.[14]

•Z17-S3-3, with Bragg spacings in the ratio 1:$\sqrt{3}$:2, the first order corresponding to d = 6.3 nm: this behavior strongly suggests in this case a two-dimensional hexagonal lattice of cylinders, as already claimed for other segmented PTMO ionenes.[13]

However, such a situation is no longer observed on the other zwitterionomers, even those with similar high zwitterion density since only two peaks are evident in their SAXS patterns. In spite of the good agreement of the ratios of the corresponding Bragg spacings with the theoretical values for lamellar or hexagonal morphology (see Table 1 and further discussion), the type of structure cannot be definitely ascertained on these unique grounds with the same reliability as in two previous more favorable cases. The sharp variations in the relative intensities in the two Bragg peaks which come with the change of the corresponding d Bragg ratios also support the occurrence of a phase transition. TEM micrographs of the two copolymers Z20-S3-6 and Z52-S3-6, assumed to display a lamellar and hexagonal morphology, respectively, are given in Figure 5. The first micrograph is actually consistent with a lamellar structure free from preferential orientation of the coher-

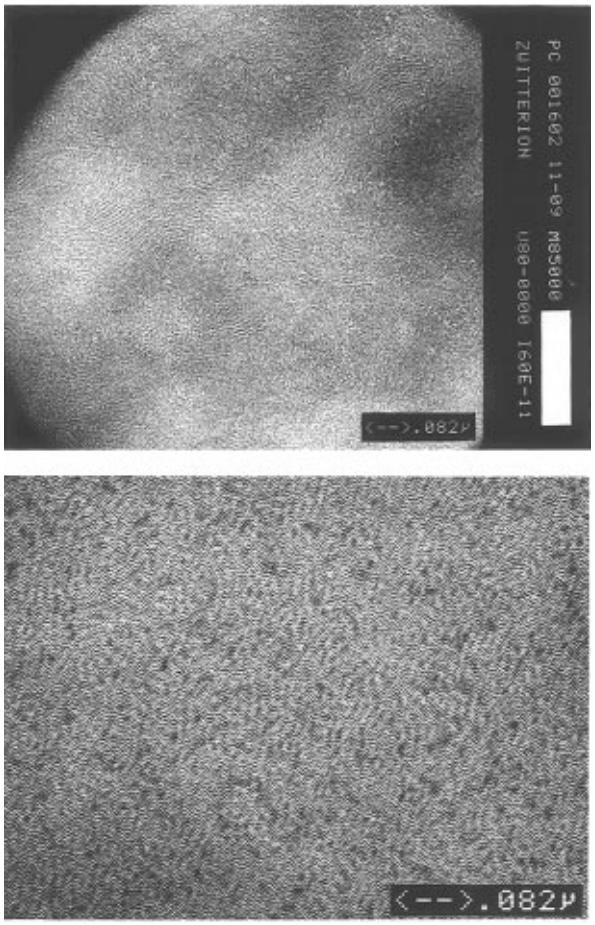

Figure 5. TEM micrographs of (a) zwitterionomer Z20-S3-6 (lamellar morphology) and (b) zwitterionomer Z52-S3-6.

ence domains. It allows us to estimate the total thickness of the lamella and thickness of the PTMO and zwitterionic layers to about 7.9, 6.7, and 1.2 nm, respectively, in good agreement with the corresponding values derived from SAXS analysis of 7.4, 6.5, and 0.9 nm (see Table 1 and discussion further in the text). Moreover, coherence domains spread out more ten lamellar periodicities and reach dimensions higher than 100 nm. The second micrograph, however, is more ambiguous and cannot be definitely ascribed to a lamellar or cylindrical structure (significantly different pictures can be obtained for a hexagonal structure according to the orientation of the image plane with respect to the cylinder axis). Thus, in order to check furthermore the proposed structures and mainly the hexagonal one, two types of complementary experiments based respectively on swelling and on uniaxial stretching of the samples were designed. Preliminary results of uniaxial streching[15] already support the previous indexation, and a more comprehensive study will be reported in a forthcoming paper. Only the swelling behavior is discussed below.

Swelling Experiments. SANS experiments were performed on zwitterionomers Z22-E2-6 and Z52-E2-6 which only differ by the length of the PTMO segments and are assumed to display a lamellar and a hexagonal morphology, respectively. Tetrahydrofuran (THF) was chosen as the swelling medium because it is a selective solvent of the PTMO chains (see further) and shows quite similar scattering length density with respect to SANS measurements (ρ(PTMO) = ρ(THF) = 0.2×10^{-10} cm^{-2}). The two zwitterionomers readily lead to physical gels in THF, with maximum equilibrium swelling ratios

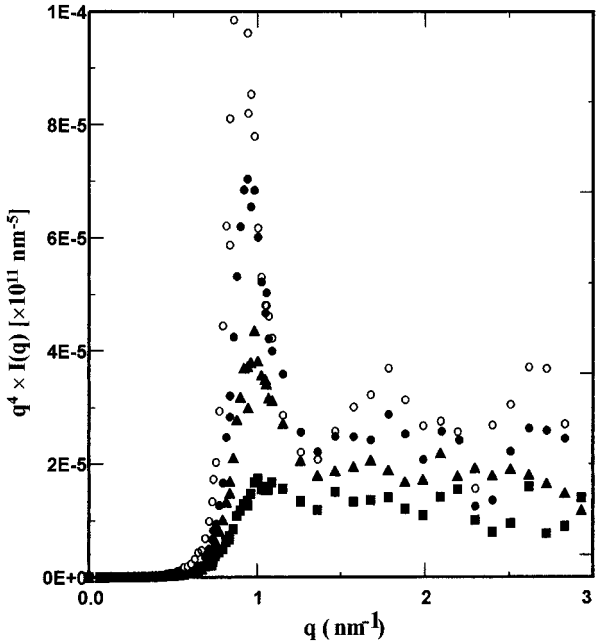

Figure 6. Porod plot of the SANS pattern of zwitterionomer Z22-E2-6 swelled in THF at various swelling ratios Q: (○) Q = 1 (Φ_B = 0.128); (●) Q = 1.3 (Φ_B = 0.099); (▲) Q = 1.5 (Φ_B = 0.080); (■) Q = 2.3 (Φ_B = 0.051).

at 25 °C of Q = 5 and 4.3 for Z22-E2-6 and Z52-E2-6, respectively ($Q = \Phi_p^{-1}$ where Φ_p is the volume fraction of the polymer in the swollen system). The SANS patterns of the Z22-E2-6 gels, given in Figure 6 and indexed according to the volume fraction of the scattering zwitterionic units in the swollen system, Φ_B, are quite representative for the two systems. They clearly show three major features: (i) The first is the persistence of the first-order diffraction peak with only weak fluctuations on its position. The variations of the corresponding Bragg spacings d with the zwitterion volume fraction are better seen in Figure 7 for the two zwitterionomers. (ii) The second is the loss of the second-order diffraction peak, even for the smallest swelling ratios, Q > 1.3, which suggests loss of long range order in the system. This is also evidenced by the broadening of the first-order diffraction peak. (iii) Moreover, these same SANS data plotted in the form of the $G(q,c)$ function (see Data Treatment) clearly show at high q (q > 2 nm^{-1}) a constant plateau value which is directly proportional to the ratio surface over volume S_p/V_p of the scattering entities: $H_2 = 2\pi(S_p/V_p) = 7.1 \pm 0.2$ and 9.0 ± 0.5 nm^{-1} for Z22-E2-6 and Z52-E2-6 gels, respectively, independent of the swelling ratio.

Thus the sorption of THF by the zwitterionomers does not result in a simple affine swelling of the initial structure, but it introduces disorder in the system. The invariance of the average correlation distance between the zwitterionic domains and of their characteristic ratios S_p/V_p can be reconciled within two types of structural model which will be discussed successively.

The first model involves a process of progressive and dilution-induced fragmentation of the organized domains essentially characterized by two features: a constant number of scattering particles N_p by unit volume, which implies that their aggregation number is a decreasing function of the swelling ratio, and the redistribution of the zwitterionic units in highly anisotropic microdomains of constant shape. Considering in this model the Porod representation $q^4\, I(q) = f(q)$, it is of special interest to analyze the variations of the

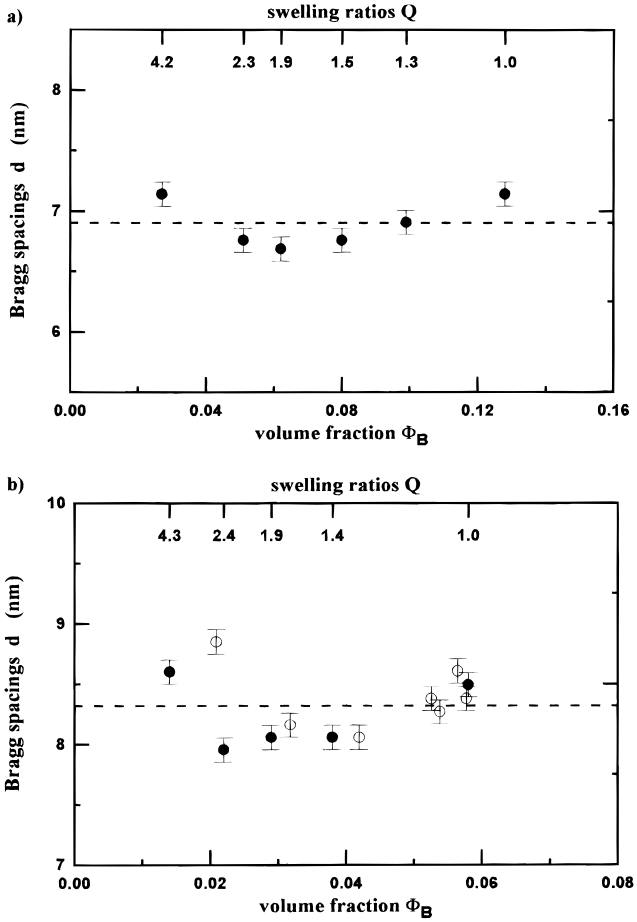

Figure 7. Variation of the Bragg spacings d of the physical gels with the volume fraction of zwitterions Φ_B in the systems (●) SANS and (○) SAXS data: (a) Z22-E2-6/THF; (b) Z52-E2-6/THF.

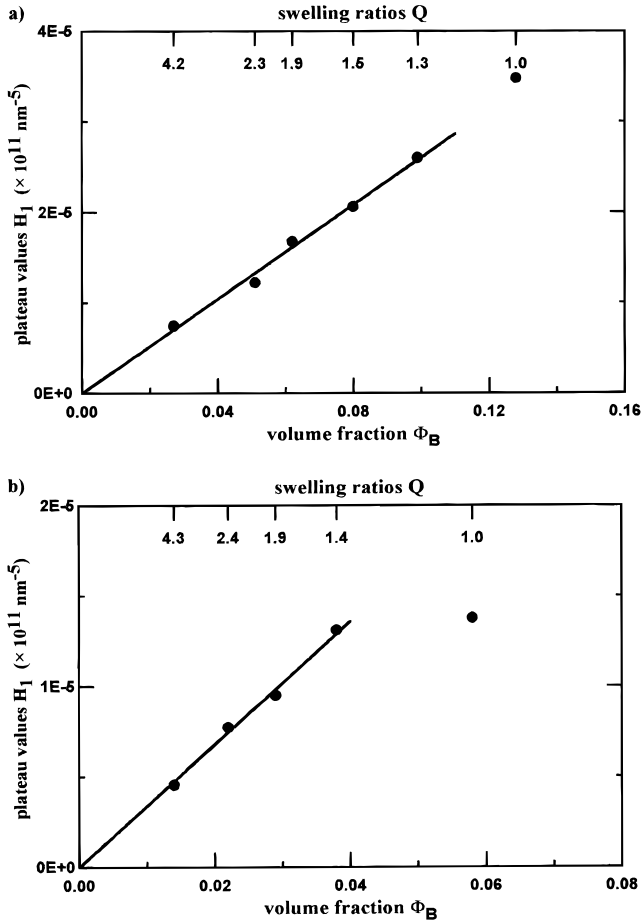

Figure 8. Variation of the plateau value H_1 with the volume fraction of zwitterions Φ_B for the physical gels (a) Z22-E2-6/THF and (b) Z52-E2-6/THF.

plateau values H_1 observed at high q with the volume fraction of the scattering zwitterions in the system Φ_B, remembering that H_1 is proportional to the total interface area per volume unit (see eq 5). In the case of highly anisotropic scattering particles, H_1 and Φ_B are linearly correlated through their lower dimension such as the height h of a thin disk of radius R or the radius R of long cylinders according to

$$\Phi_B = \frac{h \text{ or } R}{4\pi(\rho_B - \rho_A)^2} H_1 \qquad \text{disk } R >> h, \quad \text{cylinder } h >> R \quad (7)$$

Figure 8 shows the good fit of the experimental data to this correlation which allows us to derive the values of the lower dimensions of the anisotropic zwitterionic aggregates, independent of the swelling ratios: 1.7 ± 0.1 nm for Z22-E2-6 and 1.4 ± 0.1 nm for Z52-E2-6 gels. They remain compatible with those of a bifunctional zwitterionic junction carrying a $(CH_2)_6$ bridge between ammonioethoxydicyanoethenolate functions which show an intercharge distance of 0.54 nm in their extended conformation.[22] In the case of the zwitterionomer Z52-E2-6 supposed to display an initial hexagonal morphology, it would be of definite interest to analyze thoroughly the range of small swelling ratios, $Q < 1.4$, where a quasi invariance of the H_1 value is observed and remains to be explained.

The second model involves an inhomogeneous swelling of the material. Unsolvated organized domains of unchanged lattice parameters are dispersed in a THF solution of polymer chains, and their extension (coherence length) is a decreasing function of the swelling ratio. The preexistence of a rather low amount of a disordered phase in the unswollen bulk material cannot be excluded. It may be stressed that the quantitative analysis proposed in the first model still remains valid for an inhomogeneous swelling provided that the ratio of PTMO segments to zwitterionic junctions is the same in the ordered and disordered phases.

Even if they do not allow an independent check of the lamellar or hexagonal structure of the initial zwitterionomers, swelling experiments are of much interest by themselves and may be discussed on two viewpoints: stability and shape of zwitterionic aggregates.

Swelling by THF does not reduce to a simple affine deformation of the initial structure previously observed on statistical zwitterionomers. For instance, in the case of *n*-butyl acrylate zwitterionomers of the ammoniopropanesulfonate type;[24] swelling by di-*n*-butyl phthalate, a selective solvent of the acrylate matrix, is fairly similar to an isotropic homogeneous swelling of the initial liquidlike structure (no long range order before swelling) without any significant decrease of the aggregation number of the zwitterionic multiplets. The different behavior of our systems cannot result from partial solvation of the zwitterionic microdomains since 1,6-bis((dimethylammonio)ethoxydicyanoethenolate)-hexane, a model for the zwitterionic short segment, is completely insoluble in THF at room temperature[15] (solubility lower than 8 ppm, as derived from UV measurements). Weaker dipolar interactions and hence weaker cohesion of the zwitterionic microdomains for

ammonioethoxydicyanoethenolate structures may be tentatively advanced as a reasonable explanation: it is strongly supported by the solid state ^{1}H-NMR analysis of chain dynamics in the segmented PTMO, as previously described.[2] Finally, it would be of definite interest to check this structure of the physical gels by an analysis of the dependence of their elastic moduli under uniaxial deformation G on the swelling ratio Q: significant deviations from the simple power law[25] $G \propto Q^{-1/3}$ could confirm the simultaneous variations of the functionality of the cross-linking points corresponding to the decrease of the aggregation number of the zwitterionic microdomains upon dilution. Such a study is out of the scope of the present work.

On the other hand, an isotropic (spherical) shape for the zwitterionic aggregates may be unambiguously ruled out, on the basis of the independence of the Bragg spacings d as well as of the plateau values H_2 with respect to the swelling ratio. This feature is in good agreement with literature data on analogous systems. For zwitterionic semitelechelic polymers, both theoretical calculations[23] and structural analysis in solution (nonpolar solvents)[26,27] and in bulk[28,29] show that aggregation of the dipolar units likely occurs in the form of disk or tubular structures. Quite recently and in a more general way, for A_n chains bearing a few strongly interacting B groups leading to their so-called "superstrong segregation", theoretical calculations have also shown that isotropic spherical multiplets have to be discarded[10] in favor of disklike oblate ellipsoids with finite diameter and then in favor of infinite lamellar sheets as far as the χ_{AB} interaction parameter increases.

Influence of the Molecular Structure on the Spatial Organization of the Polar Microdomains. The functionality, chemical structure, and density of the short polar junctions along the segmented chain are all potential parameters of the material morphology. For all the segmented PTMO showing at least two diffraction peaks, the lamellar and the hexagonal structures were discriminated on the basis of the characteristic d_1/d_2 ratios. For the other polymers showing only one diffraction peak (liquidlike order), the corresponding Bragg spacing was considered in a first approach as a measure of the average correlation distance between the center of the scattering microdomains assumed quasi spherical, monodisperse, and distributed with a cubic local order. This very rough and oversimplified last structural model is obviously not very realistic, but it is only used as a convenient framework for a better comparison between the various copolymers. The experimental data are given in Table 1 with some characteristic geometrical parameters such as the thickness of the zwitterionic lamella (e), the radius (R) of the cylindrical or spherical polar microdomains, and the surface area available at the interface per polar short segment (S). All these parameters are easily derived from simple space-filling considerations for any given morphology, assuming quantitative segregation of the polar units, according to the relations given in the Appendix.

Three main trends may be outlined and will be discussed successively:

(i) All the zwitterionomers bearing the shorter PTMO segments of molecular weight M_n^0 in the range $(1.7-2.2) \times 10^3$, corresponding to the higher zwitterion densities ($\Phi_B > 0.12$), display a lamellar structure (see Figure 9) characterized by a thickness e of about 1.0 ± 0.1 nm for the zwitterionic layer, in good agreement

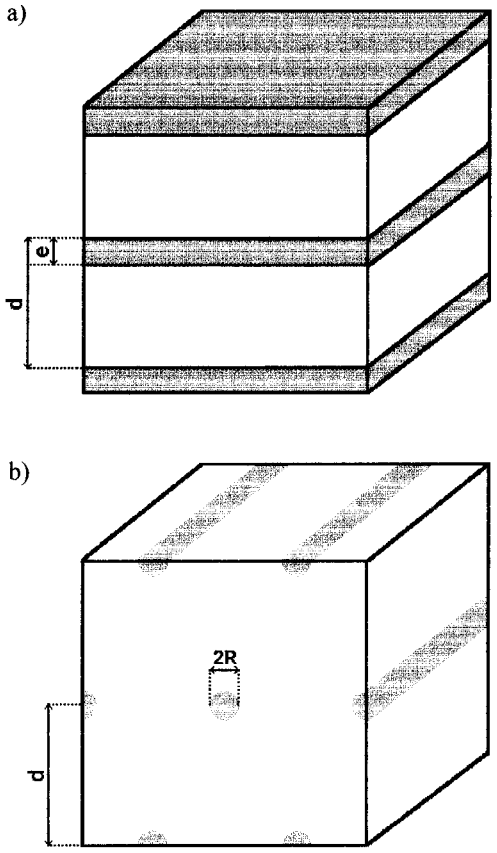

Figure 9. Schematic representation of the lamellar and hexagonal structures.

with the estimated length of the zwitterionic short segment in its all trans conformation. The only exception is Z17-53-3, where the corresponding three-order scattering pattern strongly supports a hexagonal structure: no satisfactory explanation can be provided for such a discrepancy. A lamellar morphology has already been proposed for statistical polysiloxane dizwitterionomers[30] and for PTMO ionenes ($M_n^0 \sim 1.8 \times 10^3$) where the 4,4′-bipyridinium short segments (counterions Cl^-, I^-, Br^-; weight fraction $W_I \sim 0.11-0.18$) are aggregated in disklike microdomains.[14]

(ii) All the other zwitterionomers would display a hexagonal structure where the zwitterionic units are aggregated in cylindrical microdomains: see Figure 9. Such a morphology has been claimed for a series of PTMO ionenes[13] ($M_n^0 \sim (1.8-6.6) \times 10^3$, 1,4-bis(dimethylammonio)xylene as the short segment, weight fraction $W_z \sim 0.05-0.16$). It may be stressed, however, that in this latter case, the lamellar structure (4 SAXS orders in a ratio close to the theoretical one 1:2:3:4) has been rejected in favor of the hexagonal one on the basis of an error analysis on the peak positions and of TEM micrograph pictures.

In the two previous types of long range order, the dimensions of the zwitterionic domains are barely sensitive to the nature of the difunctional dipolar junction. This feature likely results from too weak structural variations (p and x values) and from similar packing of sulfonate and dicyanoethenolate zwitterions.

(iii) The two segmented PTMO bearing only one zwitterionic site between the consecutive PTMO blocks, Z19-S3 and Z19-E2, only show a liquidlike order, with identical structural parameters: see Table 1. However, for samples Z52-S3-6 and Z52-E2-6 of similar zwitterion content ($\Phi_B = 0.053$ and 0.055, respectively) a hexagonal

morphology is actually observed. Thus, for an overall similar composition, the development of long range order appears finely tuned by the segmented chain topology: it is more favored by a regular distribution of zwitterion pairs separated by a relatively long segment than by a regular distribution of isolated zwitterions separated by shorter segments.

Zwitterionomers versus Ionenes. The three ionenes under study, I19-S-6, I19-E-6, and I22-T-6 (precursor ionene neutralized by triflate counterions), display only a liquidlike structure, and the radius of the polar multiplets (see Table 1) and their corresponding aggregation numbers N_B depend on the counterion nature, $N_B = 91$, 32, and 135, respectively. This size difference has to be considered cautiously because of the oversimplification of the structural model involved in the calculations. However, it likely remains physically meaningful and it may result from packing variations in the multiplets: steric hindrance and polarizability which monitor the Coulombic interactions within the multiplets are not the same for the alkanesulfonate, the triflate, and the more delocalized dicyanoethenolate anions. Finally, the liquidlike structure of ionenes I19-S-6 and I19-E-6 may also appear somewhat puzzling by comparison with the hexagonal or lamellar morphologies observed in fairly similar PTMO ionenes which essentially differ by their more rigid short segments of 1,4-bis(dimethylammonio)xylene[13] or bipyridinium[14] halides (Cl^-, Br^-, I^-). Note, however, that no long range order could be detected in a series of PTMO−bipyridinium ionenes neutralized by triflate counterions,[34] in good agreement with our own results on the homologous ionene I22-T-6.

The lack of long range order in these ionenes is a striking difference with the lamellar morphology observed for the homologous zwitterionomers of identical composition and identical structure of the charged sites. Obviously, the higher number of PTMO segments in the ionene chain (by a factor of about 2) does not favor an efficient development of long range order because of a higher number of segment locking interfaces. It seems, however, difficult to ascribe the difference between the two types of homologous segmented chains only to this contribution. Directed dipolar interactions between zwitterions of very high dipole moment cannot be considered as strictly equivalent to Coulombic interactions between homologous ion pairs. According to molecular mechanics and quantum chemical calculations, the aggregation of low molecular weight monofunctional zwitterions likely involves antiparallel placement of the dipolar moieties in their extended conformation ($\mu \sim 24-31$ D, corresponding to intercharge distances ~0.5−0.64 nm in our case) to form anisotropic disklike or tubelike structures.[23] Ion pairs may obviously be considered as dipolar moieties, but with significantly lower intercharge distances and dipole moments since the individual ions may come in close contact: see, for instance, the dipole moments in the range 10−17 D for various tetrabutylammonium salts[31] ($\mu = 11.2$ and 17.2 D for acetate and perchlorate, respectively). Moreover, the counterion is free to move at least up to a certain degree in order to favor the lowest energy configuration for the system.[32] The packing modes and the resulting multiplet geometries should be thus different for zwitterions and ion pairs. The possible influence of the internal multiplet structure on the development of long range order cannot be excluded.[33]

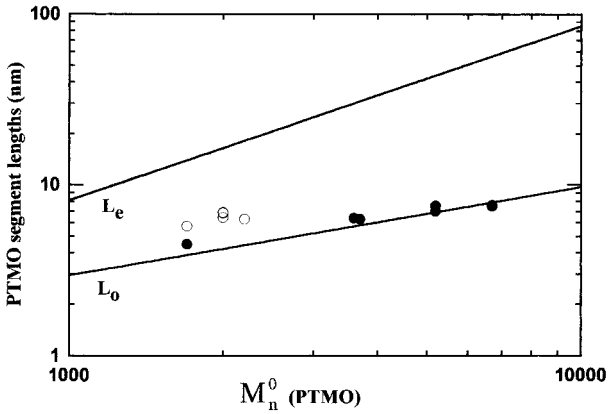

Figure 10. Variations of the experimental PTMO segment length L with its number average molecular weight M_n^0 in the bifunctional zwitterionomers: (○) lamellar structure; (●) hexagonal structure. The calculated straight lines L_e and L_0 are related to the extended and unperturbed conformations, respectively.

Chain Extension in PTMO Segmented Zwitterionomers. The problem of chain extension in ionomers remains a much debated and still controversial topic. Conflicting theoretical models have predicted either an expansion of the chain[3,4,7,32,34] as a result of ion aggregation or no change in the average chain dimensions.[35] In a parallel way, experimental studies have also proved to be contradictory.[36,37] The zwitterionomers under study are characterized by nearly monodisperse PTMO segments and a well-defined lamellar or hexagonal morphology with sharp interfaces between the zwitterionic domains and the surrounding matrix. They should allow a reliable comparison of the end to end distance L of the PTMO (N monomeric units) segments connecting neighboring zwitterionic domains with the theoretical values calculated in the two limiting cases of a fully extended or an unperturbed Gaussian conformation, L_e and L_0, respectively:

$$L_e = N\sum n_i l_i \sin(\theta_i/2) \tag{8}$$

$$L_0 = [C_\infty N\sum n_i l_i^2]^{1/2} \tag{9}$$

The parameters l_i and θ_i are related to the ith bond length and bond angle, respectively: l(C−C) = 0.153 nm, θ(C−C) = 109°; l(C−O) = 0.143 nm, θ(C−O) = 111°. The PTMO characteristic ratio C_∞ taken from the literature[36,38] is 5.7.

Figure 10 shows the variations of the calculated and experimental values of the PTMO segment end to end distances L_e, L_0, and L ($L = d - e$ and $L = 2d/\sqrt{3} - 2R$ for lamellar and hexagonal structures, respectively) with its molecular weight M_n^0. It allows us to discriminate two regimes:

(i) In lamellar structures corresponding to the shorter PTMO segments ($M_n^0 \sim 2.0 \times 10^3$), the PTMO chain appears partially but definitely extended with respect to its unperturbed state, with an average ratio $L/L_0 \sim 1.5 \pm 0.1$. In a very rough model, the PTMO chain may be considered as a central subchain of $N_0 - 2x$ monomeric units in its unperturbed state flanked at both ends by x extended terminal units at its two interfaces with the zwitterionic layers. Such an assumption leads to x values in the range 1.7−2.4 which may be compared with the number of monomeric PTMO units rigidified in the high T_g phase, as derived from the DSC structural

analysis,[2] $x \sim 2-3$. In spite of the oversimplification of the model, this good agreement may not be purely incidental.

(ii) In hexagonal structures corresponding to the longer PTMO segments ($M_n^0 > 3.6 \times 10^3$), the PTMO chain essentially appears in its unperturbed state, $L/L_0 < 1.1$.

However, it may be stressed that the absolute values of the ratio L/L_0 have to be considered cautiously for two reasons. (i) The scatter of the literature data for the characteristic ratio of PTMO:[39] for instance, calculations of L_0 using the value of the Kuhn segment[14] $b = 0.73$ nm ($L_0^2 = Nb^2$) leads to L/L_0 ratios higher by about 10%. (ii) The method of calculation of unperturbed dimensions L_0, by itself: In the analysis of the same problem, Cooper et al.[37] have critically discussed the choice of a Gaussian random coil for the conformation of PTMO chains of low molecular weights ($M_n^0 \sim 2.0 \times 10^3$) and preferred the model of a wormlike chain. The corresponding end to end distance, L_w, may be calculated using the following equation:[40]

$$L_w^2 = 2L_e q - 2q^2[1 - \exp(-L_e/q)] \qquad (10)$$

where q is the persistence length of the PTMO chain easily derived from its characteristic ratio C_∞ according to[41]

$$C_\infty = 2q/l - 1 \qquad (11)$$

where l is the average bond length. For $M_n^0 > 10^3$, the difference between L_0 and L_w always remains lower than 5% (as expected for chains of more than 100 flexible bonds), and the choice of a Gaussian random coil or of a wormlike chain for the reference unperturbed state does not change the previous conclusions.

Thus, the general trend suggested by these data is in very good agreement with that observed in the case of analogous PTMO ionenes[14,36,38] where calculations were arbitrarily performed by assuming lamellar morphology over the whole composition range: $L/L_0 \sim 1.4$ for $M_n^0 \sim 2.0 \times 10^3$, $L/L_0 < 1.1$ for $3 \times 10^3 < M_n^0 < 10^4$. Moreover, it is self-consistent with the fact that chains are more sterically constrained and thus more extended when emerging in a perpendicular direction from the surface of a lamella than radially from the convex surface of a cylindrical microdomain. The surface area available at the interface per short segment in the lamellar structure is fairly constant, $S = 0.53 \pm 0.06$ nm^2, as expected. The corresponding higher S values calculated for hexagonal structures are actually a linear increasing function of the PTMO segment molecular weight, as shown in Figure 11. This behavior strongly supports a Gaussian unperturbed conformation of the chain which can be inscribed within a sphere of radius $\propto M_n^{0.5}$ and of cross-section $\propto M_n$.

Finally, for two segmented PTMO ionomers (SO_3^-,Na^+) which only show liquidlike order, Cooper et al.[37] have directly measured the radius of gyration of the polydisperse PTMO segments ($M_n^0 = 1 \times 10^3$ and 2×10^3) and concluded to the lack of any extension with respect to their unperturbed conformation. This behavior may be tentatively reconciled with the opposite one observed in our zwitterionomers of similar PTMO segment length: in the latter case, the PTMO segments are nearly monodisperse ($M_w/M_n < 1.15$) and are organized in the more constraining lamellar structures.

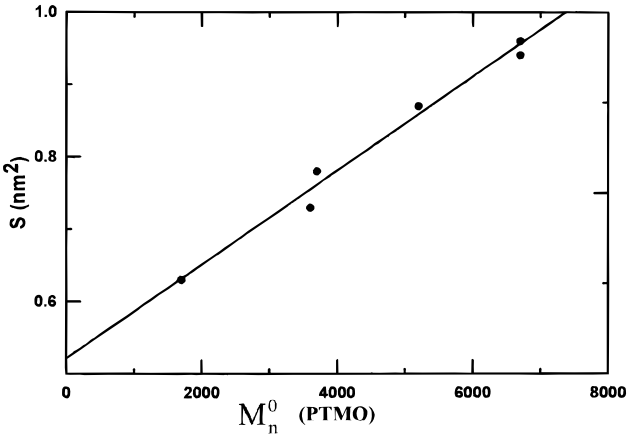

Figure 11. Variation of the surface area S available per zwitterionic junction with the number average molecular weight M_n^0 of the PTMO segment in the hexagonal structures.

Conclusion

All the segmented PTMO zwitterionomers and ionenes are microphase-separated materials, as a result of the quantitative segregation of the dipolar or ionic short segments within the highly mobile and weakly polar PTMO matrix. However, only the zwitterionomers bearing bifunctional junctions display long range order. A characteristic transition from lamellar to hexagonal structures occurs when decreasing the zwitterion density along the chain for a PTMO segment length of about 3×10^3 (corresponding to a volume fraction of dizwitterionic junctions Φ_B of about 0.10). The very typical difference between the zwitterion and the homologous ion-pair structures in their abilities for the development of long range order in fairly homologous segmented chains is worth stressing. However, the comparison of our results with literature data on similar systems clearly shows that it is not yet possible to settle a series of well-defined criteria for the development of long range order: if a narrow molecular weight distribution of the segment is a necessary but not sufficient condition, the structure of the polar junction (chemical nature, rigidity, steric hindrance, functionality) and its density along the chain definitely also appear as important parameters. Moreover, the potential influence of the overall chain length and polydispersity cannot be ruled out: a higher number of PTMO segments should likely restrict long range order as a result of slower kinetics to reach the thermodynamic equilibrium corresponding to an ordered structure.

It would be thus of definite interest to develop further studies on segmented zwitterionomers and ionenes, for instance on the following points:

- analysis of the complete phase diagram, by analogy with the well-known behavior of block copolymers,[42] with special emphasis on the search for potential bicontinuous cubic phases between the lamellar and hexagonal phases, for a possible transition from a hexagonal to a micellar cubic structure for the lowest dipolar content, and for the dipolar threshold concentration for phase separation.
- systematic chemical variations of the zwitterionic and ion-pair chemical structures for a better grounded comparison between zwitterionomers and ionenes and to estimate the minimum polarity contrast between the matrix and the polar junctions necessary for microphase separation.
- study of the influence of uniaxial stretching on the structure, with special emphasis on the separation of

orientation and deformation effects as a function of the stretching ratios.

Finally, as already suggested by the previously discussed swelling experiments in THF, these zwitterionomers and ionenes should be excellent model associative polymers for the study of self-association and physical gelation phenomena of amphipatic segmented chains in solution in nonpolar solvents.

Acknowledgment. We gratefully acknowledge A. Brulet and F. Boué for their help in the use of the spectrometer PAXE at LLB and for further valuable discussions with one of them (F.B.) and M. Audenaert and P. Coupard (Elf-Atochem, Serquigny) for the transmission electron microscopy experiments. We are greatly indebted to the reviewers for their fruitful suggestions.

Appendix: Calculation of Some Geometrical Parameters from SAXS Data for Three Different Structures

For any A_xB_y biphasic system showing quantitative segregation of the B units in monodisperse domains, the geometric parameters such as the thickness e of the B layer of a lamellar structure, the radius R of the B cylinders distributed over a bidimensional hexagonal lattice, the radius R of the B spheres distributed over a tridimensional cubic lattice and finally the surface area S available per B unit at the interface are directly derived from the Bragg spacing d (first diffraction order), the volume fraction of B units Φ_B in the system and their molar volume V_B:

structure	e or R	S
lamellar	$e = \Phi_B d$	$2V_B/eN_a$
hexagonal	$R = (2\Phi_B d^2/\pi\sqrt{3})^{1/2}$	$2V_B/N_aR$
cubic (simple)	$R = (3\Phi_B d^3/4\pi)^{1/3}$	$3V_B/N_aR$

where N_a is the Avogadro number

References and Notes

(1) Grassl, B.; Galin, J. C. *Macromolecules* **1995**, *28*, 7035.
(2) Grassl, B.; Meurer, B.; Scheer, M.; Galin, J. C. *Macromolecules* **1997**, *30*, 236.
(3) Eisenberg, A.; Hird, B.; Moore, B. *Macromolecules* **1990**, *23*, 4098.
(4) Nyrkova, I. A.; Khokhlov, A. R.; Doi, M. *Macromolecules* **1993**, *26*, 3601.
(5) Ehrmann, M.; Mathis, A.; Meurer, B.; Scheer, M.; Galin, J. C. *Macromolecules* **1992**, *25*, 2253.
(6) Gingreau, C. Thesis, L. Pasteur University, Strasbourg, 1993.
(7) Eisenberg, A.; King, M. *Ion Containing Polymers*; Academic Press: New York, 1977.
(8) MacKnight, W. J.; Earnest, T. R. *J. Polym. Sci., Macromol. Rev.* **1981**, *16*, 41.
(9) Mauritz, K. A. *J. Macromol. Sci., Rev. Macromol. Chem. Phys.* **1988**, *C28*, 65.
(10) Semenov, A. N.; Nyrkova, I. A.; Khokhlov, A. R. *Macromolecules* **1995**, *28*, 7491.
(11) Lee, D. C.; Register, R. A.; Yang, C. Z.; Cooper, S. L. *Macromolecules* **1988**, *21*, 998.
(12) Visser, S. A.; Cooper, S. L. *Macromolecules* **1991**, *24*, 2584.
(13) Feng, D.; Wilkes, G. L.; Meir, C. M.; Stark, J. E. *J. Macromol. Sci., Chem.* **1989**, *A26*, 1151.
(14) Hashimoto, T.; Sakurai, S.; Morimoto, M.; Nomura, S.; Kohjiya, S.; Kodaira, T. *Polymer* **1994**, *35*, 2672.
(15) Grassl, B. Thesis, L. Pasteur University, Strasbourg, 1995.
(16) Dreyfuss, P. Poly(tetrahydrofuran), Gordon & Breach Science Publishers: New York, 1982; p 159.
(17) Guillon, D.; Mathis, A.; Skoulios, A. *J. Phys. Fr.* **1975**, *36*, 695.
(18) *Small Angle X-Ray Scattering*; Glatter, O., Kratky, O., Eds.; Academic Press: London, 1982.
(19) Cotton, J.; Auvray, L.; Auroy, P. In *Neutron, X-Ray and Light Scattering*; Lindner, P., Zemb, Th., Eds.; Elsevier: Amsterdam, 1991.
(20) Cabane, B. In *Surfactant Solutions: New Methods of Investigation*; Zana, R., Ed.; M. Dekker: New York, 1987.
(21) Feng, D.; Venkateshwaran, L. N.; Wilkes, G. L.; Leir, C. M.; Stark, J. E. *J. Appl. Polym. Sci.* **1989**, *38*, 1549.
(22) Galin M.; Chapoton A.; Galin J. C. *J. Chem. Soc., Perkin Trans. 2* **1993**, 545.
(23) Bredas, J. L.; Chance, R. R.; Silbey, R. *Macromolecules* **1988**, *21*, 1633.
(24) Galin, M.; Mathis, A.; Galin, J. C. *Macromolecules* **1993**, *26*, 4919.
(25) Bastide, J.; Candau, S. J. In *Physical Properties of Polymeric Gels*; J. Wiley: New York (in press).
(26) Davidson, N. S.; Fetters, L. J.; Funk, W. G.; Graessley, W. W.; Hadjichristidis, N. *Macromolecules* **1988**, *21*, 112.
(27) Wang, Z. G. *Langmuir* **1990**, *6*, 928.
(28) Fetters, L. J.; Graessley, W. W.; Hadjichristidis, N.; Kiss, A. D.; Pearson, D. S.; Younghouse, L. B. *Macromolecules* **1988**, *21*, 1644.
(29) Shen, Y.; Safinya, C. R.; Fetters, L.; Adam, M.; Witten, T. *Phys. Rev. A* **1991**, *43*, 1886.
(30) Graiver, D.; Litt M.; Baer E. *J. Polym. Sci., Chem. Ed.* **1979**, *17*, 3573 and 3625.
(31) Grunwald, E.; Highsmith S.; Ting-Po, I. In *Ions and Ion Pairs in Organic Reactions*; McSzwarc, M., Ed.; J. Wiley: New York, 1974; Vol. 2, p 447.
(32) Dreyfus, B. *Macromolecules* **1985**, *18*, 284.
(33) Vlaic, G.; Williams, C. E.; Jerome, R.; Tant, M. R.; Wilkes, G. L. *Polymer* **1988**, *29*, 173.
(34) Forsman, W. C. *Macromolecules* **1982**, *15*, 1032.
(35) Squires, E.; Painter, P.; Howe, S. *Macromolecules* **1987**, *20*, 1740.
(36) Feng, D.; Wilkes, G. L. *Macromolecules* **1991**, *24*, 6788.
(37) Visser, S. A.; Pruckmayr, G.; Cooper, S. L. *Macromolecules* **1991**, *24*, 6769.
(38) Feng, D.; Wilkes, G. L.; Lee, B.; McGrath, J. E. *Polymer* **1992**, *33*, 526.
(39) Brandrup, J.; Immergut, E. H. *Polymer Handbook*, 2nd ed.; John Wiley & Sons: New York, 1975.
(40) Kratky, O.; Porod, G. *Recl. Trav. Chim. (Pays Bas)* **1949**, *68*, 1106.
(41) Flory, P. J. *Statistical Mechanics of Chain Molecules*; Interscience: New York, 1969; p 111.
(42) Bates, F. S. *Science* **1991**, *251*, 898.

MA960880V